Morphology and magnetic properties of submonolayer Gd films

M. Gajdzik, T. Trappmann, C. Sürgers, and H. v. Löhneysen
Physikalisches Institut, Universität Karlsruhe, D-76128 Karlsruhe, Germany
(Received 30 January 1997; revised manuscript received 4 August 1997)

We report on scanning tunneling microscopy (STM) measurements on ultrathin Gd films in the thickness range $0.5 \leqslant d_{\mathrm{Gd}} \leqslant 10$ ML [1 monolayer (ML)=2.89 Å] grown on a Y (0001) buffer layer at substrate temperatures $T_s = 473$ K and $T_s = 573$ K. The magnetic properties were investigated on these films capped with a 100-Å Y layer with the transverse magneto-optical Kerr effect. A ferromagnetic signal was found down to the sub-ML regime $d_{\mathrm{Gd}} \approx 0.5$ ML for $T_s = 473$ K. In this regime, the STM images show a lateral growth of ML thick Gd islands of hexagonal shape. The depression of the Curie temperature T_C follows a power law $\Delta T_C \propto d_{\mathrm{Gd}}^{-\lambda}$ with an exponent $\lambda \approx 1$ up to $d_{\mathrm{Gd}} \approx 3$–5 ML, where λ changes to $\lambda = 1.6$. This transition is also observed in the same thickness range for the exponent β of the magnetization M. [S0163-1829(98)02306-6]

I. INTRODUCTION

In three-dimensional (3D) ferromagnets, salient magnetic properties such as the Curie temperature or the spontaneous magnetization and its temperature dependence depend only weakly on structural defects. In thin films however, particularly in ultrathin films down to the monolayer and submonolayer range, these properties become structurally sensitive.[1] Scanning tunneling microscopy (STM) offers the chance to elucidate the interplay between morphology and magnetism in ultrathin films, and considerable progress has been achieved recently in understanding important aspects of thin-film magnetism from STM studies.[2–5]

So far, the majority of these investigations have been done on transition metal films to understand the detailed influence of the film morphology on the establishment of long-range ferromagnetic order. Similar studies for rare-earth films such as Gd are rather scarce, although there have been many studies on the magnetic properties of Gd films. Most of the work has been done on Gd films grown on W(110),[6–9] where a strong influence of the growth conditions on the structural and magnetic properties has been reported. This has been further confirmed by a recent STM investigation.[10]

We have shown previously that (0001)-oriented Gd films of high epitaxial quality prepared on an Y(0001) buffer layer on top of a Nb(110) surface at substrate temperatures $T_s =$ 573 K and capped with a 100-Å Y film exhibit long-range ferromagnetic order down to the monolayer range.[11] It is therefore highly desirable to characterize the growth of these films by STM and relate the film morphology to the magnetic properties. In this paper we report on the structural characterization of ultrathin Gd films by STM and the magnetic behavior of these films prepared at different T_s capped with a 100-Å Y layer; namely, the thickness dependence of the Curie temperature and the spontaneous magnetization. Although the magnetic measurements are performed on a Y/Gd/Y sandwich the STM results give insight into the morphology of the buried Gd layer.

II. EXPERIMENT

All samples have been prepared by electron-beam evaporation in ultrahigh vacuum (UHV) on a clean Nb(110) single crystal oriented to a precision of $\pm 0.5°$ as described elsewhere.[11] In the present study additional surface cleaning of the Nb substrate was done *in situ* in UHV by several cycles of sputtering with 1.5-keV Ar^+ ions and subsequent annealing.[12] After each step the result of the cleaning procedure was controlled by Auger electron spectroscopy (AES). Surface investigations have been done *in situ* in a separate chamber at room temperature with a commercial UHV scanning tunneling microscope. One of the most important conditions for scanning tunneling microscopy is a well-prepared tunneling tip. We used electrochemically etched tungsten tips which were cleaned *in situ* by heating to ≈1273 K and subsequent Ar^+ sputtering. This procedure yields a sharp tip with a radius of curvature down to about 30 nm.[13] The STM images were taken in the constant-current mode with the bias voltage applied to the sample and the tip grounded.

A 750-Å Y (0001) buffer layer was deposited on the *in situ* cleaned Nb (110) surface at $T_s = 873$ K as described in Ref. 11. The film thickness was controlled by a quartz oscillator monitor calibrated via x-ray diffraction on Gd/Y superlattices. All thicknesses mentioned in this paper are nominal thicknesses. The resulting stepped Y surface [Fig. 1(a)] follows essentially the morphology of the Nb surface with an average terrace width of ≈500 Å due to the substrate miscut of ≈0.5°. Adatom islands are only found on the largest steps indicating that adatom diffusion is generally sufficient for the atoms to reach a step edge.

In Fig. 1(a) few defects but a bright (i.e., apparently higher) seam at the step edges can be observed. This seam is attributed to oxygen impurities which are adsorbed during transfer from the evaporation chamber to the STM chamber or are segregated from the Nb substrate during evaporation.[14] About 5% oxygen impurities on the Y surface are detected with AES. In some cases we successfully achieved atomic resolution on the Y surface [Fig. 1(b)] confirming the hexagonal symmetry and the epitaxial growth in the (0001) direction. At first sight the defect in the upper left corner seems to be a Y vacancy. However, this is unlikely because of the high vacancy diffusion at the surface at room temperature.[15] More likely, this defect is attributed to an oxygen adsorbate which can be imaged either as an apparent depression or a protrusion depending on the tunneling voltage.[16]

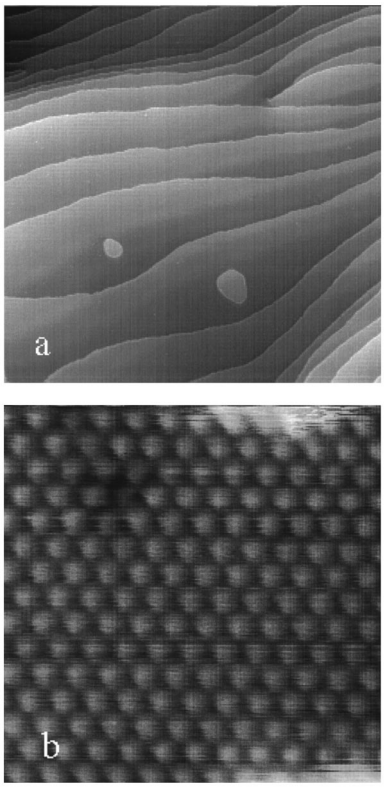

FIG. 1. STM images of the (a) Y(0001) surface (3000 $\times$3000 Å^2, I=1 nA, U=0.1 V), and (b) the Y(0001) surface with atomic resolution (46$\times$46 Å^2, I=4.4 nA, U=28 mV).

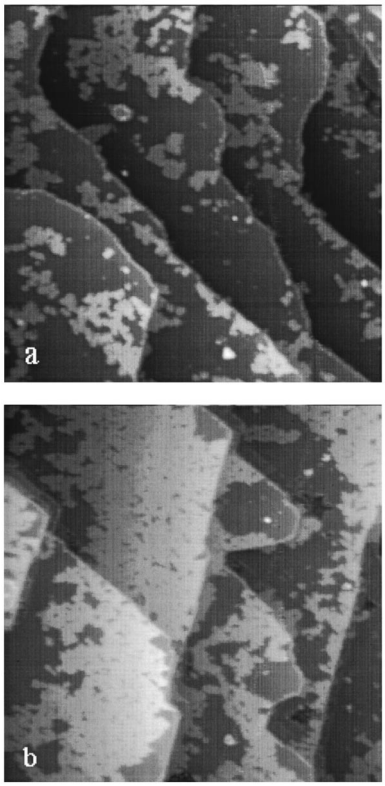

FIG. 2. STM images (1000$\times$1000 Å^2, I=1–2 nA, U=0.1 V) of Gd on Y with (a) d_{Gd}=2 Å and (b) d_{Gd}=4 Å prepared at T_s=573 K.

Gd was evaporated at a rate of 0.02 Å/s at T_s=473 K or T_s=573 K (with a delay of 10 min after each completed Å to promote surface diffusion and layer-by-layer growth[12]). After the STM studies all samples were covered with a 100-Å Y protective layer at T_s=473 K to prevent them from oxidation in air (exposure time 10–15 min) during the transfer to a ^{4}He cryostat. This 100-Å layer was sufficient as confirmed by Auger depth profiling on an air-oxidized sample. The magnetization was measured by means of the magneto-optical Kerr effect in transverse geometry (t-MOKE) in the temperature range from 3 to 300 K as described in detail elsewhere.[11,17] This method is sensitive enough to obtain a sufficiently strong signal even from submonolayer Gd films capped with Y as shown below. However, our experimental setup (polarizer-compensator-sample-analyzer configuration) did not allow an absolute measurement of the Kerr signal, i.e., magnetization.

III. RESULTS AND DISCUSSION

We first studied the growth of Gd on Y at a substrate temperature T_s=573 K for comparison with the previously published magnetic measurements on films prepared at that T_s.[11] Since both elements grow in the hcp (0001) orientation with a very small lattice mismatch in the basal plane ($\approx$0.5%) they cannot be distinguished by topology only. However, both elements can be identified in STM due to a strong chemical contrast originating from electronic surface states.[12,18] Depending on the voltage applied to the sample the STM images are either dominated by Gd or Y. All images in this paper were taken at a voltage of U=+0.1 V where Gd atoms appear ''higher.''

Samples prepared at T_s=573 K show long-range ferromagnetic order only down to d_{Gd}=3.5 Å (nominal coverage Θ_n=1.2).[11] STM studies of these samples (Fig. 2) reveal that for T_s=573 K the effective Gd coverage is much smaller than Θ_n. Here and in the following the coverage is expressed in the units of monolayers (ML). For a nominal thickness d_{Gd}=2 Å [Fig. 2(a)] the measured effective coverage Θ_{eff}=0.36 (which is also in agreement with the AES data) is certainly less than expected from the Θ_n=0.69. In fact, no large continuous Gd regions are found explaining the fact that no long-range ferromagnetism was observed for nominal thicknesses $d_{\mathrm{Gd}}<$3.5 Å. It has to be noted that the apparently higher (i.e., brighter) Gd patches seen in Fig. 2(a) are not situated on top of the Y surface but in fact are embedded in the uppermost Y layer which was proved by varying the sample voltage.[12] For d_{Gd}=4 Å we would expect coverage of the entire surface, but Fig. 2(b) still shows some areas of uncovered Y although there is no evidence for Gd islands with 2-ML thickness. The obvious explanation is that a substantial fraction of the deposited Gd atoms has diffused into the few topmost Y layers during deposition. The strong dilution with Y leads to a suppression of ferromagnetism.

Figure 3 shows STM images for several samples prepared at the lower T_s=473 K. It is remarkable that these samples show a ferromagnetic transition even down to a half-monolayer coverage Θ_n=0.52 [d_{Gd}=1.5 Å, Fig. 3(b)], as shown in Fig. 4 where magnetization curves at 5–7 K obtained with the t-MOKE are plotted.

Samples with d_{Gd}=1.1 Å (Θ_n=0.38, average island size only 5000 Å^2) do not show any magnetic signal down to T

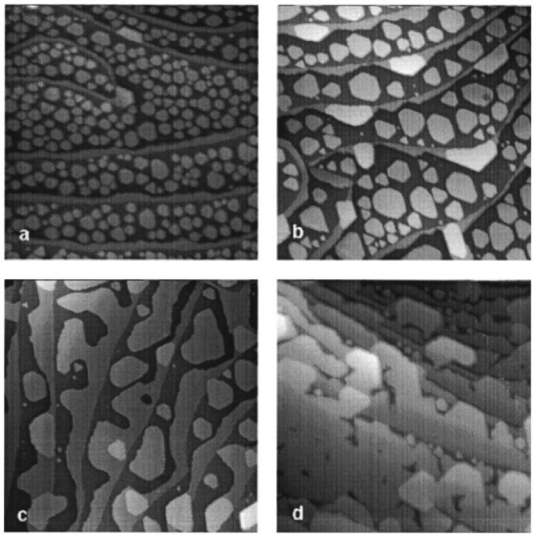

FIG. 3. STM images (2000×2000 Å^2, $I=1$–2 nA, $U=0.1$ V) of Gd on Y prepared at $T_s=473$ K with (a) $d_{\mathrm{Gd}}=1.1$ Å, (b) $d_{\mathrm{Gd}}=1.5$ Å, (c) $d_{\mathrm{Gd}}=2.3$ Å, and (d) $d_{\mathrm{Gd}}=2.9$ Å.

$=3$ K. This latter finding is in nice agreement with the data for $T_s=573$ K where a nominal coverage of $\Theta_n=0.69$ leads to a similar average island size (due to interdiffusion) not showing a ferromagnetic signal [cf. Fig. 2(a)]. Furthermore, we note that for $T_s=473$ K the islands are situated on the Y terraces (Fig. 3) compared to $T_s=573$ K where they are embedded in the surrounding Y as mentioned above (cf. Fig. 2).

For the 1.5-Å sample ($T_s=473$ K) we observe an average Gd-island size (averaged over 2000×2000 Å^2) of 12 300 Å^2 [Fig. 3(b)]. For this sample, a magnetic signal is clearly

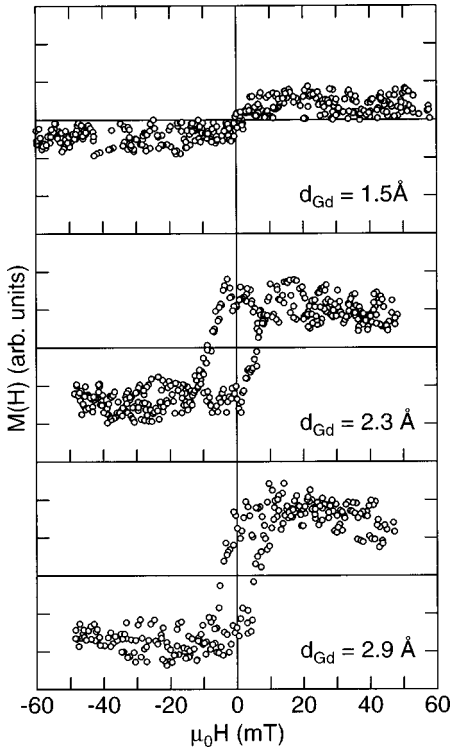

FIG. 4. Hysteresis loops, i.e., magnetization M vs applied magnetic field $\mu_0 H$, obtained by MOKE measurements on Gd films ($T_s=473$ K) with $d_{\mathrm{Gd}}=1.5$ Å, 2.3 Å, and 2.9 Å at $T=5$–7 K.

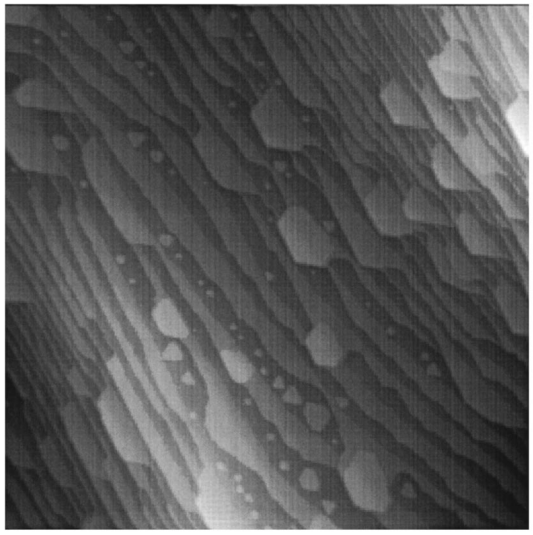

FIG. 5. STM image (same parameters as in Fig. 3) for $d_{\mathrm{Gd}}=1.5$ Å with an intentional misorientation of 1.5°.

seen (Fig. 4). However, the magnetization curves $M(H)$ of this sample do not show any hysteresis, contrary to samples with a higher Gd coverage indicating a coercivity $\mu_0 H_c \approx 10$ mT (Fig. 4). This suggests that the signal for the 1.5-Å sample presumably arises from superparamagnetism of the Gd islands as found earlier for 2D-Fe islands grown on CaF_2/Si(111) with an average island size smaller than 3200 Å^2 (Ref. 19). However, a coercivity $\mu_0 H_c < 5$ mT for the 1.5-Å sample cannot be excluded because of the small magnetic signal and poor data resolution. Figure 3 clearly shows that Gd accumulates at the terrace steps in the form of stripes, in addition to forming islands. These stripes are not attributed to oxygen impurities mentioned above but to the evaporated Gd as confirmed by STM spectroscopy and AES measurements.[18]

The fact that the stripes are already present for $d_{\mathrm{Gd}}=1.1$ Å where no ferromagnetic signal is observed, supports that it arises from islands exceeding a threshold size. This is further corroborated by the following experiment. A sample with an intentional misorientation of 1.5° leads to an average terrace width of about 50 Å only. After evaporation of nominal 1.5-Å Gd at $T_s=473$ K only stripes of Gd are observed (Fig. 5). These samples do not show a ferromagnetic signal down to $T=3$ K as checked by MOKE. Therefore we can firmly conclude that the ferromagnetic contribution in the MOKE signal of the 1.5-Å Gd film is due to the larger islands seen in Fig. 3(b). For higher Gd coverages the islands join with the stripes at terrace edges [Fig. 3(c)] until for $d_{\mathrm{Gd}}=2.9$ Å $=1$ ML the Y surface is nearly completely covered. Perfect coverage is not achieved due to the onset of Gd growth in the second layer. From the nearly rectangular shape of our hysteresis curves we infer that samples with $d_{\mathrm{Gd}}>1.5$ Å show no out-of-plane magnetization as predicted for uncovered Gd films on W(110) with $d_{\mathrm{Gd}}<8$ ML (Ref. 20).

Having discussed the growth of submonolayer Gd films we now turn to the magnetic properties of these films capped with a 100-Å Y layer. First, the dependence of the Curie temperature T_C on film thickness d_{Gd} will be discussed for samples prepared at the optimum $T_s=473$ K. T_C was determined by two methods: (a) The magnetization $M(T)$ was

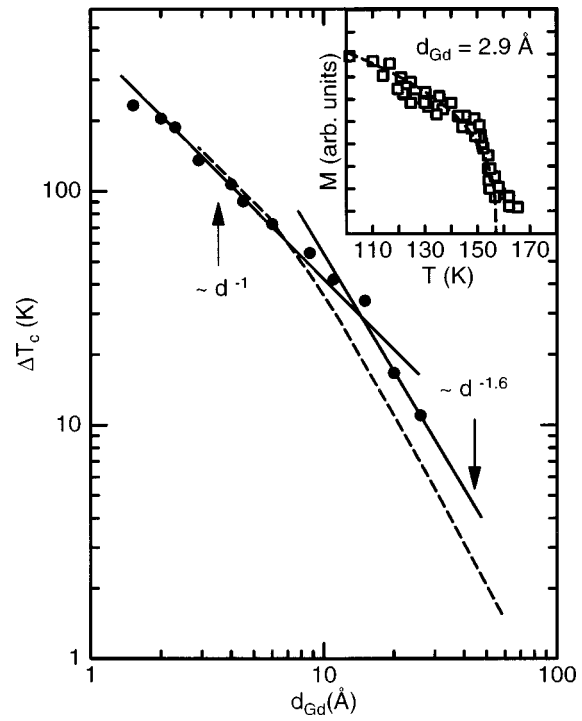

FIG. 6. Suppression ΔT_C of the Curie temperature as a function of film thickness d_{Gd}. Filled circles: experimental data (T_s=473 K); dashed line: generalized mean-field theory for Heisenberg ferromagnets (Ref. 29). Solid lines illustrate $d_{\mathrm{Gd}}^{-1.6}$ and d_{Gd}^{-1} dependence. Inset shows the determination of T_C by extrapolating the magnetization $M(T)$ measured in a small external field B=10 mT to $M(T_C)$=0 for d_{Gd}=2.9 Å (dashed line). For this sample the extrapolation is nearly identical to a power-law fit (mentioned in the text) with β=0.23.

measured in a small external field B=10 mT and extrapolated to $M(T_C)$=0. T_C was taken from the inflection point in the $M(T)$ curve, above which the magnetization is dominated by the paramagnetic tail caused by the applied field. The inset in Fig. 6 shows an example. (b) T_C' was obtained with the Arrott-plot method where T_C' is given by the temperature at which the M^2 vs H/M plot intersects the origin.[21] The values obtained by the two methods are in good agreement, for instance, T_C=281±3 K, 250±3 K, 157±5 K compared to T_C'=279.5±0.5 K, 248.5±0.5 K, 155±1 K for d_{Gd}=26, 11, and 2.9 Å, respectively. The error in the determination of T_C increases with decreasing film thickness mainly due to the increasing scatter of the data, i.e., decreasing magnetic signal. $\Delta T_C = T_C(\infty) - T_C(d_{\mathrm{Gd}})$ is shown in the main frame of Fig. 6, with $T_C(\infty)$=292.5 for Gd.[9] The error in the T_C determination corresponds to the symbol size in the log-log plot.

Theoretically, the thickness dependence of the Curie temperature $T_C(d_{\mathrm{Gd}})$ is expected to obey a power law due to finite-size effects:[22–24]

$$\Delta T_C = T_C(\infty) - T_C(d_{\mathrm{Gd}}) \propto d_{\mathrm{Gd}}^{-\lambda},$$

where the exponent λ depends on the dimensionality and universality class of the system. For Ising systems λ is related to the critical exponent ν for the magnetic correlation length via $\lambda = 1/\nu$ (Refs. 22–24). Hence λ_{3D}=1.587 and λ_{2D}=1. Applying this relation to 3D-Heisenberg ferromagnets leads to λ=1.418. However, theoretically it was shown that a small uniaxial anisotropy can change the critical exponents of the 3D-Heisenberg system to become Ising-like.[25] Similarly, in two dimensions where no long-range ferromagnetic order can occur in a Heisenberg system, any weak uniaxial anisotropy is able to induce a phase transition of Ising character.[26,27]

For thick films with d_{Gd}>11 Å we find an exponent λ =1.6 corresponding either to the 3D-Ising or the 3D-Heisenberg model, bearing in mind that the difference between both models of the value of λ is small. This exponent is in agreement with previous results of samples prepared at the higher T_s=573 K (Ref. 11) and with ac-susceptibility data of 5–100 ML Gd on W(110), where the $T_C(d_{\mathrm{Gd}})$ behavior was described with the 3D Ising value.[7] In contrast, for thin films with d_{Gd}<11 Å the exponent changes to λ=1 corresponding to the 2D-Ising model. The fact that this change in the exponent was not observed in our previous study[11] is probably due to the stronger scatter in the T_C values of the earlier films caused by the interdiffusion occurring at T_s=573 K as mentioned above.

Absolute values for the T_C reduction with decreasing film thickness have been calculated earlier by a generalized mean-field theory for hexagonal Heisenberg ferromagnets.[29] These results are included in Fig. 6. Other calculations of the absolute critical temperatures employing a Páde approximation[23] or Monte Carlo simulations[28] are valid for cubic Ising systems and the predicted values of $T_C(d)$ depend on various assumptions and boundary conditions. However, our data are superficially compatible with the calculated T_C values for d=1 ML [e.g., T_C(1 ML) ≈0.5$T_C(\infty)$=146 K for Gd] as well as with the calculated thickness where the exponent changes (d≈4 ML=11.6 Å for Gd).[23,28]

A transition due to a dimensional crossover from 3D to 2D behavior was already observed for Gd films on W(110) for thicknesses between 15 and 5 ML in the critical exponent γ of the magnetic susceptibility,[8] for Ni on W(110) between 7 and 5 ML in the exponent λ (Ref. 30), and for Ni films on Cu at 7–12 ML in the critical exponent β of the magnetization.[31]

In order to further investigate a possible dimensional crossover we determined the critical exponent β of the magnetization. This is often done by using a method first demonstrated by Dürr *et al.*,[32] where T_C is determined by maximizing the range of $\log(1-T/T_C)$ over which the data in a $\log M$ vs $\log(1-T/T_C)$ plot represent a straight line with slope β. For the present data this method is somewhat arbitrary concerning the choice of T_C and the fitting range caused by the scatter of the data. This is due to the paramagnetic tail and the small MOKE signal from the buried magnetic layer. Alternatively, we decided to vary T_C by ±1 K around the value obtained with the Arrott-plot method and determined the exponent β for each value of T_C, thereby giving an estimate for the error in the determination of β.

Figure 7 shows the magnetization $M(T)$ of three films measured in B=10 mT vs reduced temperature $t=1-T/T_C$ for different values of T_C on a log-log plot. Within the limited accuracy and limited t range, the data appear to follow a

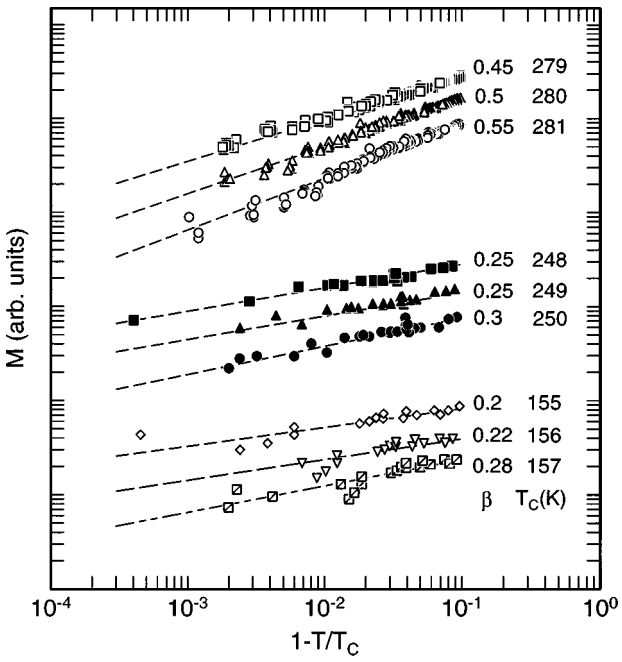

FIG. 7. Log-log plot of the spontaneous magnetization $M(B=10\ \mathrm{mT})$ vs reduced temperature $(1-T/T_C)$ for samples prepared at $T_s=473$ K. The dashed lines illustrate a behavior $M\propto(1-T/T_C)^{\beta}$ for the indicated Curie temperature $T_C(d_{\mathrm{Gd}})$. Sample thickness is $d_{\mathrm{Gd}}=26$, 11, and 2.9 Å (from top to bottom data set). Data are shifted vertically for clarity.

power law $M(T)\propto(1-T/T_C)^{\beta}$ with an exponent $\beta=0.5\pm0.08$ ($d_{\mathrm{Gd}}=26$ Å), $\beta=0.27\pm0.05$ ($d_{\mathrm{Gd}}=11$ Å), and $\beta=0.23\pm0.05$ ($d_{\mathrm{Gd}}=2.9$ Å). Although the error in the determination is large, a sudden transition of the exponent from ≈0.5 for $d_{\mathrm{Gd}}>11$ Å to ≈0.25 for $d_{\mathrm{Gd}}\leqslant11$ Å can be identified when data from all samples are taken into account. In particular, β is almost constant in the thin-film region. Assuming $\beta=0.25$ for $d_{\mathrm{Gd}}>11$ Å yields unreasonably low Curie temperatures which are not consistent with the measured $M(T)$ behavior.

Thus a change of β occurs in the same d_{Gd} range as that of λ, although the absolute values of β are incompatible with the theoretical values for 2D-Ising ($\beta=0.125$) and 3D-Ising or Heisenberg ferromagnets ($\beta=0.33-0.37$) (Refs. 33–35) expected from the above mentioned $T_C(d)$ behavior.

For thick films, our result $\beta\approx0.5$ is identical to the mean-field value but definitely larger than both the 3D-Heisenberg value $\beta=0.375$ obtained previously from *in situ* MOKE measurements on a 300-Å Gd film on W (110) (Ref. 21) and the value $\beta=0.37$–0.38 for bulk Gd.[36] A possible explanation might be a rounding of the transition, for instance due to a distribution of Curie temperatures caused by fluctuations of the film thickness on a large lateral scale. A broadening of the transition has been taken into account in previous thin film studies for Gd/W(110) (Ref. 37) and Fe/W(110) (Ref. 43) by assuming a Gaussian distribution of Curie temperatures around an average T_C. However, in the present work the paramagnetic tail does not allow an unambiguous analysis of the data in this respect.

In the thin film region the value $\beta\approx0.25$ is in agreement with results obtained on several transition metal films such as Fe on Au(100) (Ref. 32) and Ni on Cu (Refs. 31,38) where similar differences between the experimental and the theoretical exponents have been found. In particular, a similar behavior, i.e., a change of β from 0.45–0.5 to ≈0.25 with decreasing film thickness around $d=5$–7 ML, was observed for Ni films on Cu(100) and Cu(111).[31] It should be mentioned that real layered magnets and thin films with pure in-plane magnetic anisotropy should be considered as realizations of the 2D-XY model. Although for infinite size this model exhibits a Kosterlitz-Thouless phase transition not sustaining long-range order, the behavior is modified due to finite-size effects and $M(T)$ can be described in a restricted temperature range with a power law and an effective exponent $\beta\approx0.23$ (Ref. 39). The experimental data of a number of different films and layered magnets with in-plane anisotropy are compatible with this finite-size 2D-XY model.[31,32,38,40]

On the other hand, as pointed out by Kohlhepp *et al.*[41] the reported exponents in many cases should not be interpreted as true critical exponents, since the method for their determination varies from study to study or the temperature interval is outside the critical region. In the present case β was determined in roughly the same range of t as in the studies on Ni/Cu (Ref. 31) and Au/Fe.[32]

One possible reason for a difference in the critical behavior of our samples compared to Gd films on W(110) might be a crucial role of the substrate, i.e., Y(0001) or W(110). In addition, the Y cover layer can influence the magnetic properties compared to uncovered magnetic films. For instance, T_C of a free Fe(110) monolayer on W(110) is enhanced from 210 to 296 K when coated with Ag.[42] For the same system, an indirect interaction of electronic origin between double-layer islands mediated by the surrounding monolayer and the W substrate probably leads to a frustration of magnetic order for certain coverages.[5] Thus, for submonolayer coverages of Gd in Y/Gd/Y sandwiches the indirect exchange between different islands via the Ruderman-Kittel-Kasuya-Yosida (RKKY) interaction might change the magnetic behavior compared to uncovered Gd films. This has to be investigated further. In summary, we find a common change of the exponents β and λ at a thickness $d_{\mathrm{Gd}}\approx11$ Å. β is similar to values found in a large number of different magnetic films, although it may not be considered as a true critical exponent. We mention that for an accurate analysis of the critical behavior of monolayer and submonolayer films more elaborate surface sensitive techniques such as spin-polarized low-energy electron diffraction have to be used, as very recently employed for an Fe (110) monolayer on W(110).[43]

IV. CONCLUSION

Thin epitaxial Gd films were grown on Y in (0001) orientation by electron-beam evaporation and studied with STM and the magneto-optical Kerr effect. Comparison of film morphology and magnetic properties yields an optimum growth temperature of $T_s=473$ K as a compromise between atomically flat layer growth requiring high T_s and suppression of interdiffusion requiring low T_s. Samples prepared at this temperature show a ferromagnetic signal down to half a monolayer coverage ($d_{\mathrm{Gd}}=1.5$ Å) indicating that an average Gd island size of about 12 000 Å^2 is sufficient to establish

long-range ferromagnetic order within the island. For the covered Gd monolayer we observe $T_C = 155\ \mathrm{K} = 0.53\ T_C(\infty)$. Samples with an average island size of only 5000 $\mathrm{Å}^2$ show no ferromagnetic signal. It is open whether this is simply due to the lack of sensitivity of our t-MOKE experiment (limited by the Y cap layer) or, possibly, to superparamagnetism in the present temperature range. The role of the RKKY interaction between islands (mediated through the Y conduction electrons on the substrate and the cap layer) needs to be investigated.

The depression of the Curie temperature varies as $\Delta T_C \propto d_{\mathrm{Gd}}^{-\lambda}$ with an exponent $\lambda = 1$ for $d_{\mathrm{Gd}} \leqslant 11$ Å (4 ML) changing to $\lambda = 1.6$ for thicker films. This is attributed to a dimensional crossover from 2D- to 3D-Ising or 3D-Heisenberg ferromagnetism. Furthermore, a significant change of the exponent β of the magnetization M is observed in the same thickness range. However, the experimental data for β do not agree with the theoretical values for the Ising system but are in agreement with experimental values found for band ferromagnets with in-plane magnetization.

[1] U. Gradmann, in *Handbook of Magnetic Materials*, edited by K. H. J. Buschow (Elsevier, Amsterdam, 1993), Vol. 7/1, pp. 1–96.

[2] J. de la Figuera, J. E. Prieto, C. Ocal, and R. Miranda, Phys. Rev. B **47**, 13 043 (1993).

[3] J. A. Stroscio and D. T. Pierce, J. Vac. Sci. Technol. B **12**, 1789 (1994).

[4] J. Giergel, J. Kirschner, J. Landgraf, J. Shen, and J. Woltersdorf, Surf. Sci. **310**, 1 (1994).

[5] H. J. Elmers, J. Hauschild, H. Fritzsche, G. Liu, U. Gradmann, and U. Köhler, Phys. Rev. Lett. **75**, 2031 (1995).

[6] D. Weller, S. F. Alvarado, W. Gudat, K. Schröder, and M. Campagna, Phys. Rev. Lett. **54**, 1555 (1985).

[7] M. Farle, K. Baberschke, U. Stetter, A. Aspelmeier, and F. Gerhardter, Phys. Rev. B **47**, 11 571 (1993).

[8] A. Aspelmeier, F. Gerhardter, and K. Baberschke, J. Magn. Magn. Mater. **132**, 22 (1994).

[9] K. Baberschke, M. Farle, and M. Zomack, Appl. Phys. A: Solids Surf. **44**, 13 (1987).

[10] E. D. Tober, R. X. Ynzunza, C. Westphal, and C. S. Fadley, Phys. Rev. B **53**, 5444 (1996).

[11] M. Gajdzik, U. Paschen, C. Sürgers, and H. v. Löhneysen, Z. Phys. B **98**, 541 (1995).

[12] T. Trappmann, Ph.D. thesis, Physikalisches Institut, Universität Karlsruhe, 1997.

[13] J. P. Ibe, P. P. Bey, S. L. Brandow, R. A. Brizzolare, N. A. Burnham, D. P. DiLella, K. P. Lee, C. R. K. Marrian, R. J. Colton, J. Vac. Sci. Technol. A **8**, 3570 (1990).

[14] C. Sürgers and H. v. Löhneysen, Appl. Phys. A: Solids Surf. **54**, 350 (1992).

[15] T. Michely, T. Land, U. Littmark, and G. Comsa, Surf. Sci. **272**, 204 (1992).

[16] L. Ruan, F. Besenbacher, I. Stensgaard, and E. Laegsgaard, Phys. Rev. Lett. **70**, 4079 (1993).

[17] U. Paschen, C. Sürgers, and H. v. Löhneysen, Z. Phys. B **90**, 289 (1993).

[18] T. Trappmann, M. Gajdzik, C. Sürgers, and H. v. Löhneysen, Europhys. Lett. **39**, 159 (1997).

[19] M. R. Scheinfein, K. E. Schmidt, K. R. Heim, and G. G. Hembree, Phys. Rev. Lett. **76**, 1541 (1996).

[20] G. André, A. Aspelmeier, B. Schulz, M. Farle, and K. Baberschke, Surf. Sci. **326**, 275 (1995).

[21] M. Farle, W. A. Lewis, and K. Baberschke, Appl. Phys. Lett. **62**, 2728 (1993).

[22] M. E. Fisher and A. E. Ferdinand, Phys. Rev. Lett. **19**, 169 (1967).

[23] G. A. T. Allan, Phys. Rev. B **1**, 352 (1970).

[24] C. Domb, J. Phys. A **6**, 1298 (1973).

[25] D. Jasnow and M. Wortis, Phys. Rev. **176**, 739 (1968).

[26] M. Bander and D. L. Mills, Phys. Rev. B **38**, 12 015 (1988).

[27] R. P. Erickson and D. L. Mills, Phys. Rev. B **43**, 11 527 (1991).

[28] K. Binder, Thin Solid Films **20**, 367 (1974).

[29] L. Valenta, Phys. Status Solidi **2**, 112 (1962).

[30] Yi Li and K. Baberschke, Phys. Rev. Lett. **68**, 1208 (1992).

[31] F. Huang, M. T. Kief, G. J. Mankey, and R. F. Willis, Phys. Rev. B **49**, 3962 (1994).

[32] W. Dürr, M. Taborelli, O. Paul, R. Germar, W. Gudat, D. Pescia, and M. Landolt, Phys. Rev. Lett. **62**, 206 (1989).

[33] Shang-Keng Ma, *Modern Theory of Critical Phenomena* (Benjamin, New York, 1976).

[34] F. Y. Wu, Rev. Mod. Phys. **54**, 235 (1982).

[35] D. C. Mattis, *The Theory of Magnetism II* (Springer-Verlag, Berlin, 1985); C. N. Yang, Phys. Rev. B **7**, 480 (1973).

[36] A. R. Chowdhury, G. S. Collins, and C. Hohenemser, Phys. Rev. B **33**, 6231 (1986).

[37] U. Stetter, M. Farle, K. Baberschke, and W. G. Clark, Phys. Rev. B **45**, 503 (1992); M. Farle and W. A. Lewis, J. Appl. Phys. **75**, 5604 (1994).

[38] C. A. Ballentine, R. L. Fink, J. Araya-Pochet, and J. L. Erskine, Phys. Rev. B **41**, 2631 (1990).

[39] S. T. Bramwell and P. C. W. Holdsworth, J. Phys.: Condens. Matter **5**, L53 (1993).

[40] S. T. Bramwell and P. C. W. Holdsworth, J. Appl. Phys. **73**, 6096 (1993).

[41] J. Kohlhepp, H. J. Elmers, S. Cordes, and U. Gradmann, Phys. Rev. B **45**, 12 287 (1992).

[42] M. Przybylski and U. Gradmann, Phys. Rev. Lett. **59**, 1152 (1987).

[43] H. J. Elmers, J. Hauschild, and U. Gradmann, Phys. Rev. B **54**, 15 224 (1996).